ADVANCED FUNCTIONAL MATERIALS
www.afm-journal.de

Strategy for Enhancing the Dielectric Constant of Organic Semiconductors Without Sacrificing Charge Carrier Mobility and Solubility

*Solmaz Torabi, Fatemeh Jahani, Ineke Van Severen, Catherine Kanimozhi, Satish Patil, Remco W. A. Havenith, Ryan C. Chiechi, Laurence Lutsen, Dirk J. M. Vanderzande, Thomas J. Cleij, Jan C. Hummelen, and L. Jan Anton Koster**

Current organic semiconductors for organic photovoltaics (OPV) have relative dielectric constants (relative permittivities, ε_r) in the range of 2–4. As a consequence, Coulombically bound electron-hole pairs (excitons) are produced upon absorption of light, giving rise to limited power conversion efficiencies. We introduce a strategy to enhance ε_r of well-known donors and acceptors without breaking conjugation, degrading charge carrier mobility or altering the transport gap. The ability of ethylene glycol (EG) repeating units to rapidly reorient their dipoles with the charge redistributions in the environment was proven via density functional theory (DFT) calculations. Fullerene derivatives functionalized with triethylene glycol side chains were studied for the enhancement of ε_r together with poly(*p*-phenylene vinylene) and diketopyrrolopyrrole based polymers functionalized with similar side chains. The polymers showed a doubling of ε_r with respect to their reference polymers in identical backbone. Fullerene derivatives presented enhancements up to 6 compared with phenyl-C_{61}-butyric acid methyl ester (PCBM) as the reference. Importantly, the applied modifications did not affect the mobility of electrons and holes and provided excellent solubility in common organic solvents.

1. Introduction

Organic semiconductors, thanks to their versatility, promise for larger scale, lower cost and easier production of electronic devices as compared to their inorganic counterparts. Upon growing demands for renewable energy, the photovoltaic application of organic semiconductors has received a great deal of attention over the past few decades. To realize large scale commercialization, the power conversion efficiency is one of the most important features that should be improved for organic photovoltaics (OPV). In contrast to inorganic photovoltaics where the absorption of light leads to the formation of free charge carriers, in OPV excitons (bound electron and hole pairs) are created upon excitation by light. This is mainly due to the low dielectric constant of current OPV materials where electrons and holes cannot overcome their binding energy, which exceeds the thermal energy at room temperature. Taking this fact into account, bulk heterojunction (BHJ) solar cells were designed in which exciton dissociation is facilitated at the interface of so called donor-acceptor materials bearing favorable ionization potential-electron affinity for exciton dissociation.[1,2] Upon the introduction of the BHJ concept, a turning point was achieved in the progress map of OPV followed by impressive efficiency enhancements approaching to the values over 10%. This improvement has been achieved due to the vast amount of research dedicated to morphology, band structure and device design optimization. Nevertheless, the dielectric constant enhancement of organic materials captured less attention in these optimization efforts, which demands more research being devoted to this issue.

S. Torabi, F. Jahani, Dr. R. W. A. Havenith, Dr. R. C. Chiechi, Prof. J. C. Hummelen, Dr. L. J. A. Koster
Zernike Institute for Advanced Materials
University of Groningen
Nijenborgh 4, 9747 AG, Groningen
The Netherlands
E-mail: l.j.a.koster@rug.nl

F. Jahani, Dr. R. W. A. Havenith, Dr. R. C. Chiechi, Prof. J. C. Hummelen
Stratingh Institute for Chemistry
University of Groningen
Nijenborgh 4, 9747 AG, Groningen, The Netherlands

Dr. I. Van Severen, Prof. D. J. M. Vanderzande, Prof. T. J. Cleij
Institute for Materials Research (IMO)
Hasselt University
Martelarenlaan 42, 3500, Hasselt, Belgium

DOI: 10.1002/adfm.201402244

C. Kanimozhi, Prof. S. Patil
Solid State and Structural Chemistry Unit
Indian Institute of Science
560012, Bangalore, India

Dr. R. W. A. Havenith
Ghent Quantum Chemistry Group
Department of Inorganic and Physical Chemistry
Ghent University
Krijgslaan 281 (S3) B-9000, Ghent, Belgium

Dr. L. Lutsen, Prof. D. J. M. Vanderzande
IMEC, IMOMEC Associated Laboratory
Wetenschapspark 1, Diepenbeek, Belgium

Prof. T. J. Cleij
Maastricht Science Programme
Maastricht University
P.O. Box 616, 6200 MD, Maastricht, The Netherlands

In a simulation study, Koster et al.[3] have predicted efficiencies of more than 20% by taking an increased relative dielectric constant (relative permittivity, ε_r) up to 10 into account. The enhancement of ε_r up to frequencies of GHz can diminish loss processes in OPV devices originating from Coulomb interactions between oppositely charged carriers as follows:

a) Bimolecular recombination is reversely proportional to ε_r and occurs within ≈µs timescale.[4] An increased ε_r in the ≈MHz range, therefore, leads to a reduced bimolecular recombination rate hence improved charge carrier extraction. The reduced bimolecular recombination enables the production of OPV devices with thicker films for better light harvesting.[5] Moreover, the thicker films will be favorable for upscaling the OPV technology for printing processes. b) Increasing ε_r up to ≈GHz range can lead to a reduced exciton binding energy regarding exciton lifetime (ca. 10^{-9} s).[6] c) The lifetime of the charge transfer exciton is in ≈ns time domain.[7,8] A better screening for the charge transfer state can result from increased ε_r.[9,10] d) The increased ε_r reduces the singlet-triplet energy splitting which allows for smaller band offsets without relaxation to the triplet state.[11] The smaller band offset leads to the increased open circuit voltage. To sum up, an enhancement of ε_r in the GHz range is adequate to address the major loss factors of the photocurrent originating from Coulomb interactions considering the timescale of the loss processes.

In optimized OPV cells ca. 100% internal quantum efficiency has been reported[12] however, it is worth noting that a significant open circuit voltage loss as a direct consequence of the band offset between the donor and acceptor compounds is still required for current low dielectric constant OPV materials. Moreover, the recombination in optimized BHJ systems is minimized at the cost of the reduced thickness of the active layer, hence the loss of light absorption efficiency.[5]

Therefore, tailoring organic materials for enhanced ε_r is a viable route for efficiency enhancement of current OPV systems while potentially benefiting other applications of organic semiconductors that currently suffer from their poor dielectric properties. In a more ambitious perspective, the enhancement of ε_r for organic materials can rule out the need for the BHJ structures upon a reduction of the exciton binding energy, directing the progressive pathway of OPV to a new milestone.

To date, only very few attempts at increasing the dielectric constant of organic semiconductors have been published.[13–16] Non-synthetic approaches such as physically mixing organic semiconductors with high-ε_r molecules or ion doping seem to be straightforward yet less likely to keep the absorption, transport and morphology unaffected. In a recent study, the physical addition of known high-ε_r molecules to a donor material has led to a reduced exciton binding energy, at the cost of significantly lower mobility and absorption.[15] Ion doping, another approach, can lead to an undesirable phase separated morphology of the donor-acceptor network.[16] In addition, ionic polarizations are not fast enough to screen Coulomb forces even within the timescale of the slowest loss processes such as bimolecular recombination. Breselge et al.[13] introduced triethylene glycol (TEG) side chains in a poly(*p*-phenylene vinylene) (PPV) derivative and showed an enhancement of ε_r. When blended with a fullerene derivative, this polymer yielded enhanced charge dissociation as compared with a less polar PPV derivatives.[14] However, the BHJ solar cell did not present efficiency enhancement reportedly due to the incompatible polarities of the donor and acceptor leading to the formation of large domains in the donor-acceptor network.[13] Therefore, in order to provide better mixing for the donor-acceptor blend it is beneficial to functionalize both components with identical polarities. Moreover, when the whole medium consists of donors/acceptors with enhanced ε_r, loss processes arising from Coulomb interaction become unfavorable.

Here we enhance ε_r of both fullerene derivatives and conjugated polymers through compatible functionalization approaches. For this purpose, we choose to use pendant groups bearing higher polarities without modifying the π-conjugated system, so as not to affect the mobility or band gap. The dipoles in these pendant groups should be able to freely rotate even at relatively high frequencies (≈GHz). We show that ethylene glycol repeating units fit these criteria and yield high dielectric constant organic semiconductors.

2. Materials

The nomenclature used in this manuscript is as following: EG = ethylene glycol, TEG = chains consisting two or three ethylene glycol repeating units.

Molecular dynamic studies on poly(ethylene glycol) (PEG) have confirmed their high chain flexibility and rapid motion of polar components.[17] EG and TEG yield ε_r values in the range of 5–40 in the liquid phase at drive frequencies of 1–20 GHz.[18] According to density functional theory (DFT) calculations (B3LYP/6–31G**) applied for a model TEG chain (**Figure 1**), using GAMESS-UK,[19] rotation around the H_2C-CH_2 and H_2C-O bonds can be very fast at room temperature. The rotational profiles (Table S1, Supporting Information) around these bonds show two low barriers of ca. 0.11 and ca. 0.08 eV for H_2C-CH_2 and H_2C-O rotations and larger barriers of ca. 0.35 and ca. 0.29 eV respectively (**Figure 2**a). The activation energy of 0.11 eV corresponds to a reaction rate of 0.95×10^9 s^{-1} at 175K according to Equation (1).[20]

$$k_{rate} = \frac{k_b T}{h} \exp\left(-\frac{\Delta G}{RT}\right) \quad (1)$$

where k_{rate} is the reaction rate, k_b, h and R are Boltzmann, Planck and gas constants respectively, T is the temperature and ΔG is the Gibbs free energy difference. Thus the rotation of angles ϕ between ca. 75° and ca. 285° of all bonds at low temperatures occurs readily. Full rotation is still active at 175K to overcome the barrier of 0.35 eV. The reaction rates of 1.7×10^{11} s^{-1} and 1.7×10^7 s^{-1} correspond to the activation energies of 0.11 eV and 0.35 eV respectively at 298K. Hence, at room temperature, rotations of ϕ between ca. 75° and ca. 285° are

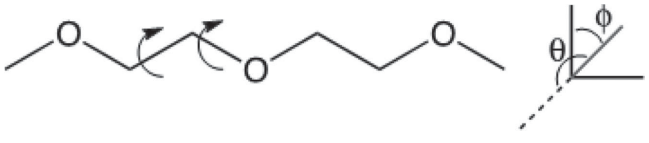

Figure 1. Repeating units of EG. Indicated are the rotations around the H_2C-CH_2 and H_2C-O bonds, and the axes of the direction of the dipole moment with respect to the molecule (θ, ϕ).

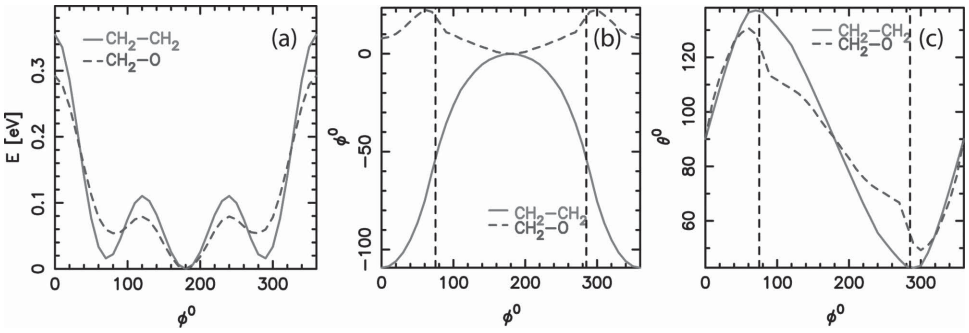

Figure 2. a) The energy with respect to the minimum as a function of the dihedral angle of the H_2C-CH_2 and H_2C-O bonds, b) the angle θ of the dipole moment as a function of the dihedral angle of the H_2C-CH_2 and H_2C-O bonds, and c) the angle ϕ of the dipole moment as a function of the dihedral angle of the H_2C-CH_2 and H_2C-O bonds.

active in GHz frequency-domain and full rotation in MHz range occurs readily. During these rotations, the magnitude of the dipole moment barely changes, but the direction of this dipole moment changes considerably (Figure 2b,c).

The swiftness and flexibility of TEG chains can provide easier reorientations for dipole moments, and thus potentially increase ε_r when being added to donors or acceptors in the GHz range. The water solubility of EGs is another advantage which brings about new possibilities towards water processable OPV.

To follow the effect of EG side chains on the dielectric constant of three important OPV materials, a set of fullerene derivatives and polymers functionalized with TEG side chains were studied (**Figure 3**). Fullerene derivatives are known as the most efficient acceptors in OPV and show excellent electron transport properties.[21] In order to enhance the dielectric constant, TEG side chains were added to C_{60}, to obtain the fullerene derivatives PTEG-1 and PTEG-2 (Figure 3c,d).[22] To differentiate the role of TEG on the dielectric constant of fullerene derivatives, an analogous fullerene derivative (PP) without TEG side chains (Figure 3b) was synthesized.[22] The influence of TEG side chains was studied for diketopyrrolopyrrole (DPP) and PPV based polymers as well. The former shows very good ambipolar transport yielding field effect mobility exceeding 10^{-2} $cm^2V^{-1}s^{-1}$.[23] It also has an absorption spectrum extending to the near infrared region. The latter lies in a well-studied class of polymers for a wide range of electronic applications.[24] 2DPP-OD-OD, the studied DPP based polymer, was used as the reference compound for 2DPP-OD-TEG in which two of the side chains of the monomer were TEG substituted (Figure 3e,f). Poly[2-methoxy-5-(2-ethylhexyloxy)-1,4-phenylenevinylene] (MEH-PPV) was used as the reference compound for PEO-PPV in which 2-ethylhexyloxy side chain is replaced with TEG (figure g,h). The synthetic routes to prepare PTEG-1, PTEG-2 and PP are reported in the reference 22. The synthetic routes of TEG functionalized DPP and PPV based polymers are published in references 23 and 13 respectively.

3. Determination of the Relative Dielectric Constant

A conventional experimental method to determine ε_r of solids is the parallel-plate-capacitance measurement with impedance spectroscopy. The material sandwiched between two metallic parallel electrodes is subject to a small perturbation of low amplitude AC signal with sweeping frequency usually from MHz range to tenths of Hz. The obtained impedance response is used to extract the capacitance value from

$$C^* = \frac{1}{j\omega Z^*} = \frac{-Z''}{\omega|Z|^2} + j\frac{-Z'}{\omega|Z|^2} \quad (2)$$

where $j^2 = -1$ and Z^* is defined as the impedance complex function indicating impedance value at a particular frequency. The dielectric function can then be derived from

$$\varepsilon_r^*(\omega) = \frac{C^*(\omega)}{C_0} = \varepsilon_r' - j\varepsilon_r'' \quad (3)$$

where $C_0 = \varepsilon_0 A/d$ is the capacitance of the empty capacitor, $\varepsilon_0 = 8.85 \times 10^{-12}$ Fm^{-1} is the electric permittivity of vacuum, A is the area of the material sandwiched between the electrodes and d is its thickness. The real part of the dielectric function corresponds to the relative dielectric constant, ε_r, of the material under test and the imaginary part encompasses loss mechanisms such as conductance and relaxation processes. In a real capacitor however, the measured impedance comprises the response of the all circuit elements such as contacts, junctions and feed lines. Therefore, employing a proper equivalent circuit model in which resistive or inductive effects are assigned to individual circuit elements can provide a fixed value corresponding to the capacitance through fitting over the experimental data. Nonetheless, not in all cases the capacitance response is merely associated with the dielectric properties of the bulk. In particular semiconductors, due to their certain degree of conductance, need a careful impedance measurement approach for the determination of ε_r.

The capacitance response of organic semiconductors can be influenced by the accumulation of space charge filling the bulk and interfacial trap states,[25,26] recombination processes[27] or purely conductive behavior of the bulk. Biasing the device reversely up to an extent that the active layer is almost entirely depleted from charge carriers can help the capacitance response to converge into the geometrical value $C_g = \varepsilon_0\varepsilon_r A/d$. In the presence of ionic contributions (dopants) though, the application of a reverse bias is not helpful to decouple bulk response from ionic polarizations.[28] A substantial increase in the capacitance at lower frequencies is indicative of ionic contributions, since ions are too slow to influence higher frequency impedance response.

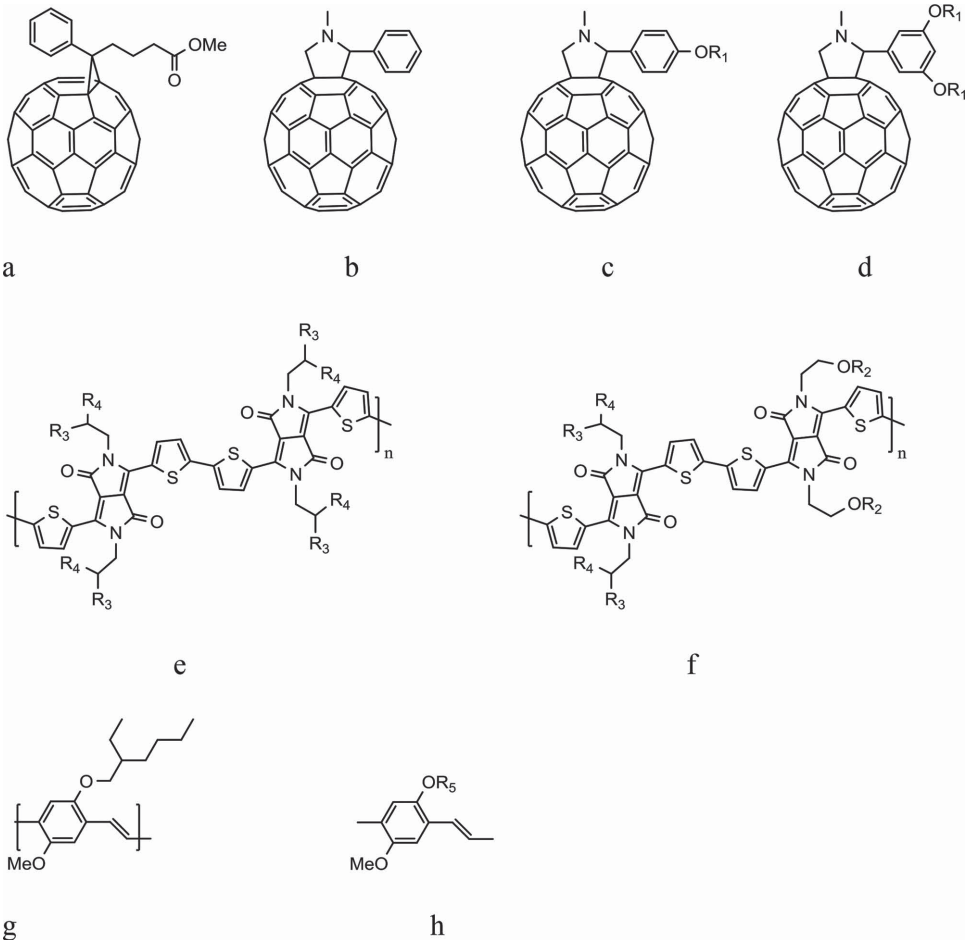

Figure 3. Chemical structures of fullerene derivatives and polymers functionalized for enhancement of ε_r and their reference compounds. a) Phenyl-C_{61}-butyric acid methyl ester (PCBM), b) PP c) PTEG-1 d) PTEG-2 e) 2DPP-OD-OD f) 2DPP-OD-TEG g) poly[2-methoxy-5-(2-ethylhexyloxy)-1,4-phenylenevinylene], h) PEO-PPV. $R_1 = (CH_2CH_2O)_3CH_2CH_3$, $R_2 = (CH_2CH_2O)_2CH_3$, $R_3 = C_8H_{17}$, $R_4 = C_{10}H_{21}$, $R_5 = (CH_2CH_2O)_3CH_3$

Computational and experimental studies[29,30] on organic films indicate that their capacitance response is dependent on the selection of the contacts as well. For instance once the film is sandwiched between two Ohmic contacts with zero built-in voltage (V_{bi}), no specific bias voltage at which the capacitance value converges to C_g is applicable. In contrast, once the film is sandwiched between two Ohmic contacts with non-zero built-in voltage, at $V<V_{bi}$ capacitance converges to C_g. Regarding injection issue, therefore, applying steady voltages well below V_{bi} can keep the charge carriers away from being injected into the device.

In this work we chose to use indium-tin-oxide (ITO) covered with poly (3,4-ethylenedioxythiophene):poly(styrenesulfonic acid) (PEDOT:PSS) as anode. All devices were tested for current–voltage characteristics to roughly estimate V_{bi}. Then we applied an AC harmonic of 10 mV in the frequency range of 100 Hz to 1 MHz superimposed on a negative DC bias to the capacitor and obtained the impedance response to find C_g. We applied several DC biases ($V<V_{bi}$) to make sure the capacitance response is not dependent on biasing. In a separate experiment we used bare ITO as anode to make sure the presence of PEDOT:PSS does not influence the results. Apart from a higher standard deviation around average values, the magnitude of the relative dielectric constant found from capacitors using bare ITO did not differ from those with PEDOT:PSS included. Comparison of their current–voltage characteristics revealed that the films spun on bare ITO bottom electrode have higher leakage current at reverse bias which accounts for higher degree of error they impose on the measurements arising from the roughness of ITO. The absence of space charge polarization effects which are extrinsic to the material's dielectric properties was verified upon testing several capacitors in different film thicknesses. For each film thickness four capacitors varying in their electrode area (0.095 cm^2, 0.1616 cm^2, 0.357 cm^2, 0.995 cm^2) were defined as a standard layout. All measured data presented perfect linear dependence of the capacitance with respect to the contact area which confirmed geometry independence of the results.

4. Determination of the Mobility

The determination of the charge carrier mobility is a crucial characterization step in organic electronics. For polymer/fullerene OPV devices, fullerene derivatives and polymers are recognized as electron and hole transporting medium

respectively. To determine the mobility of electrons/holes of fullerenes/polymers in a solar cell structure, the space charge limited current (SCLC) method was chosen. In the case of a Poole-Frenkel type mobility, the SCLC is given by[31]

$$J_{SCL} = \frac{9}{8}\varepsilon_0\varepsilon_r\mu(T)\exp\left(0.89\gamma(T)\sqrt{\frac{V_{int}}{L}}\right)\frac{V_{int}^2}{L^3} \quad (4)$$

where J_{SCL} is the electron (hole) current density, μ is zero field mobility of the electrons (holes), γ is an empirical parameter describing the field activation which depends on the temperature, V_{int} is the internal voltage (applied voltage corrected for V_{bi} and voltage drop through the series resistance of the connections) and L is the thickness of the active layer.

We designed single carrier devices by employing proper electrodes that can inject only electrons for fullerene derivatives and holes for polymers to study charge carrier mobility. By measuring current density versus voltage at different temperatures and fitting the results with Equation (4), we could find SCL mobility values of each material together with their temperature dependence. For typical charge concentrations in organic semiconductors, the charge carrier mobility exhibits an Arrhenius temperature dependence.[31]

$$\mu = \mu_\infty \exp(-\Delta/kT) \quad (5)$$

where μ_∞ is a universal value for the mobility and Δ is the activation energy. We found the activation energy from Equation (5) using the temperature dependent mobility values for each compound.

5. Results and Discussions

Table 1 lists ε_r values of all test materials determined via IS in the frequency range of 100 Hz to 1 MHz. The equivalent circuit of **Figure 4** depicts the circuit elements that modeled the impedance response of all tested samples with estimated error of less than 1% (Figure S1). The relative dielectric constant of tested materials were calculated from dividing the fitted capacitance value to C_0. To resolve the effectiveness of the functionalization of donors and acceptors with EG side chains, they were studied comparatively to their reference chemical

Table 1. The relative dielectric constant of fullerene derivatives and polymers

Fullerene Derivatives	ε_r	Tested Capacitors#
PP	3.6 ± 0.4	8
PTEG-1	5.7 ± 0.2	6
PTEG-2	5.3 ± 0.2	16
PCBM	3.9 ± 0.1	8
Polymers	ε_r	Tested Capacitors #
2DPP-OD-TEG	4.8 ± 0.1	10
2DPP-OD-OD	2.1 ± 0.1	8
PEO-PPV	6 ± 0.1	20
MEH-PPV	3 ± 0.1	12

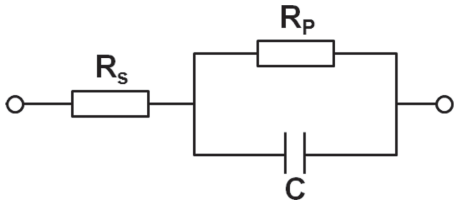

Figure 4. Equivalent circuit applied to model the experimental capacitance behavior.

structures, differing only in their side chains. PTEG-1 and PTEG-2 presented relative dielectric constants up to ca. 6 while PCBM as a widely used acceptor in OPV and PP as the reference compound yielded $\varepsilon_r \approx 4$. Likewise, the TEG-functionalized polymers were compared to their reference polymer with identical backbone, but with hydrocarbon side chains. PEO-PPV proved ε_r enhanced to ca. 6 in comparison to its reference polymer MEH-PPV with $\varepsilon_r \approx 3$. 2DPP-OD-TEG also showed the enhancement of ε_r to a value more than twice as 2DPP-OD-OD with ε_r ~2. In general, the fast change in the direction of the dipole moment can account for the high ε_r of materials with incorporated ethylene glycol chains. **Figure 5** depicts ε_r versus frequency calculated by Equation (3) while the series resistance of the contacts was subtracted from $Z^*(\omega)$. As can be seen, ε_r is weakly dependent on the frequency, which means that the obtained values are attributed to the polarization mechanisms of the materials rather than space charge polarizations or ionic movements. However, 2DPP-OD-TEG shows frequency dependence at frequencies below 10 kHz which might be due to the presence of ionic contributions. Nevertheless, ionic polarizations are less probable to remain active at frequencies higher than 10 kHz where the value of ε_r is still higher than that of the reference compound evident from Figure 5b. As is clear from the DFT calculations in section 2, the reaction rate for the change in the dipole moment direction is strongly temperature dependent for a model TEG chain. Speculated from these calculations the temperature dependence of ε_r was studied for TEG-functionalized compounds. As can be seen from **Figure 6**, ε_r of PEO-PPV and PTEG-2 is temperature dependent. However the temperature dependence for 2DPP-OD-TEG and PTEG-1 is not detectable similar to their reference compound. This might be due to the presence of steric effects in the solid state and different molecular packing of each compound that can influence the dipole moment alignments.

The enhancements of ε_r were confirmed by the measurements up to frequencies of MHz which can effectively diminish bimolecular recombination rate. Referring to the literature values[18] and our DFT calculations, one may not expect a drop of ε_r values at frequencies from 1MHz up to GHz range (at room temperature). Therefore, enhancement of ε_r is likely to contribute in diminishing the loss processes occurring in the time domain of *ns* as discussed in section 1.

The electron mobilities of PTEG-1 and PTEG-2 were determined to be 2×10^{-7} $m^2V^{-1}s^{-1}$ and 3.5×10^{-7} $m^2V^{-1}s^{-1}$ respectively with the apparent activation energy of ca. 0.2 eV (**Figure 7**a,b) which are similar to that of PCBM ($\mu_{e\text{-PCBM}} = 2 \times 10^{-7}$ $m^2V^{-1}s^{-1}$, $E_{act\text{-PCBM}} \approx 0.2$ eV).[32] For 2DPP-OD-TEG polymer the study of SCL transport yielded mobility values for both electrons and holes as 2×10^{-8} $m^2V^{-1}s^{-1}$ with

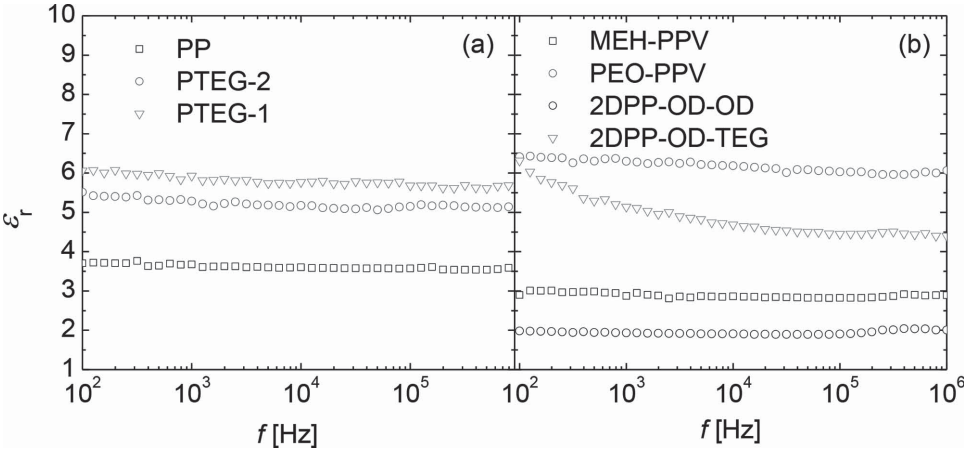

Figure 5. The relative dielectric constant of a) tested fullerene derivatives and b) polymers versus frequency.

activation energy of 0.2 eV (Figure 7d,c). These values are consistent with the results reported elsewhere.[33] **Figure 8** depicts the Arrhenius plot of obtained mobilities for extraction of the activation energy. An earlier study of the hole transport in PEO-PPV also retrieved a similar value for the hole mobility as MEH-PPV ($\mu_{\text{h-MEH-PPV}} = 1.4 \times 10^{-10}$ $m^2V^{-1}s^{-1}$).[14,34] The absence of hysteresis in the current–voltage characteristics and the quadratic dependence of the current to the voltage indicate a trap-free SCLC for the tested compounds.

6. Conclusion

In this work the relative dielectric constants of conjugated polymers and fullerene derivatives, previously restricted to the range of ca. 2–4, were boosted to the range of ca. 5 to ca. 6 via functionalization with highly polar EG side chains. Such enhancement was realized without breaking conjugation, degrading charge carrier transport, introduction of trap states and reducing solubility. Since loss processes originating from Coulomb interactions between oppositely charge carriers are not beyond the *ns* timescale, therefore the applied strategy is an effective neat method for tailoring organic compounds for a higher ε_r in the frequency range up to GHz. Additional to their great potential in enhancing the performance of OPV devices through increased ε_r, the studied fullerene derivatives and polymers can provide desirable morphologies in BHJ donor/acceptor network owing to a higher miscibility resulting from their compatible polarities. In addition, the hydrophilic character of TEG side chains, can open up new possibilities for solution processing from renewable solvents as a long term impact for tailoring state of the art organic materials.

7. Experimental Section

Device Fabrication: Commercially available glass substrates patterned with ITO in four different dimensions (0.095 cm^2, 0.1616 cm^2, 0.357 cm^2, 0.995 cm^2) were used to function as bottom electrode for capacitors. The substrates were cleaned by soap/water solution scrubbing, de-ionized water flushing, sonication with acetone and isopropyl alcohol followed by oven drying and UV-OZONE treatment. PEDOT:PSS (VP AI4083, H.C. Starck) was spin cast in ambient conditions and oven dried at 140 °C for 10 minutes. All films (fullerene derivatives or polymers) were spun from chloroform under N_2 atmosphere. Metallic top contacts including

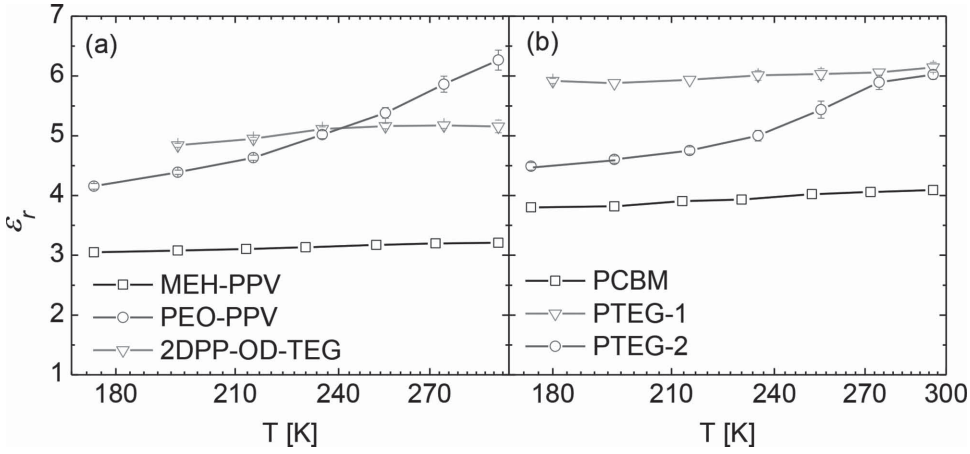

Figure 6. Temperature dependence of the relative dielectric constant. a) PTEG-1 and PTEG-2 compared with PCBM b) 2DPP-OD-TEG and PEO-PPV compared with MEH-PPV. The lines are guides to the eye.

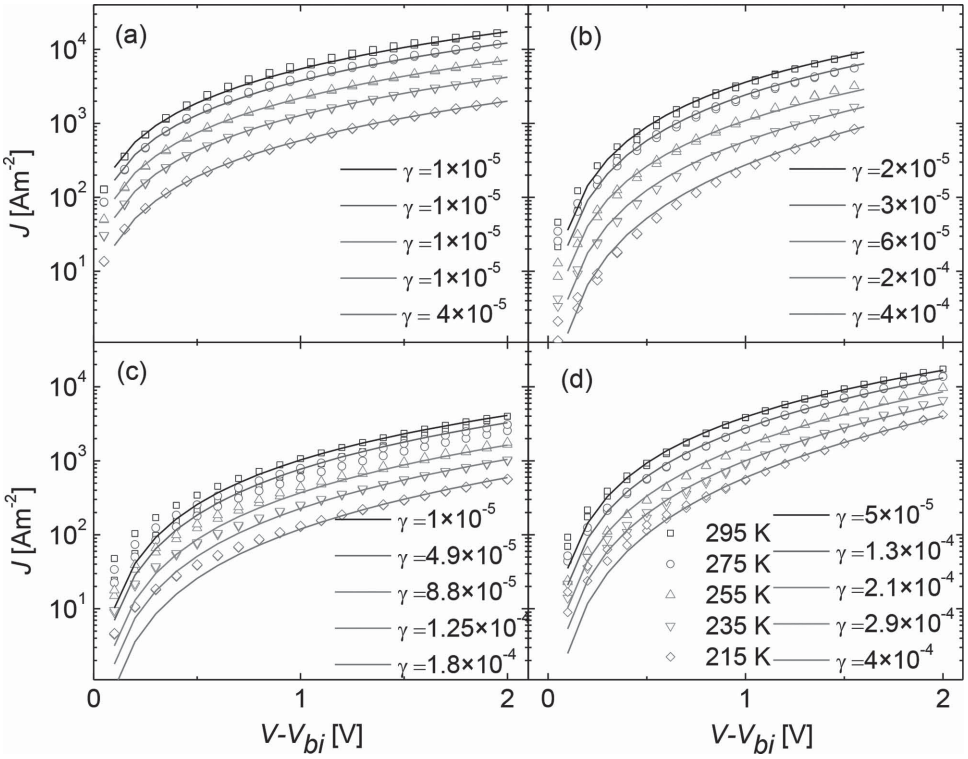

Figure 7. Steady state current voltage corrected for V_{bi} of a) Al/PTEG-2(192 nm)/Al, b) Au/PEDOT:PSS/PTEG-1(145 nm)/LiF/Al, d) Al/2DPP-OD-TEG(80nm)/Ba/Al electron-only devices and c) Au/PEDOT:PSS/2DPP-OD-TEG (96 nm)/MoO_3/Al hole-only device at temperatures ranging from 295K-215K in 20 K steps. Data (symbols) are fitted with Equation (4) (lines). The gamma values (γ[Vm^{-1}]$^{1/2}$) for each fit are provided in the legend.

interlayers (LiF(1 nm), Ba (5 nm), MoO_3 (10 nm)) were deposited at a pressure of ca. 10^{-6} mbar with thermal evaporation.

Device Characterization: Impedance spectroscopy was performed in the range of 100 Hz to 1 MHz using a Solartron 1260 impedance gain-phase analyzer with an AC drive voltage of 10 mV. Current–voltage characterization was conducted with Keithley 2400 source meter. All measurements were performed in N_2 at stable temperature.

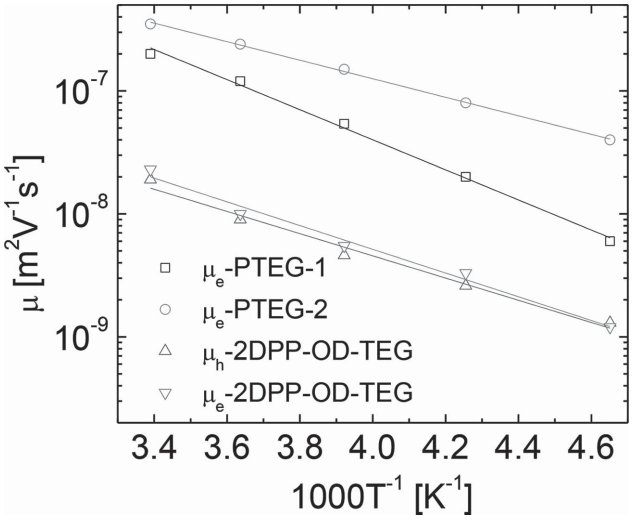

Figure 8. Mobility of charge carriers versus temperature for PTEG-2, PTEG-1 and 2DPP-OD-TEG (symbols) and corresponding Arrhenius fit (lines) yield the activation energies ~0.2 eV.

Supporting Information

Supporting Information is available from the Wiley Online Library or from the author.

Acknowledgements

L.J.A.K. acknowledges support by a grant from STW/NWO (VENI 11166). The work by S.T. and F.J.B. is part of the research program of the Foundation for Fundamental Research on Matter (FOM), which is part of the Netherlands Organization for Scientific Research (NWO). This is a publication by the FOM Focus Group 'Next Generation Organic Photovoltaics', participating in the Dutch Institute for Fundamental Energy Research (DIFFER).

Received: July 7, 2014
Published online: October 14, 2014

[1] G. Yu, J. Gao, J. C. Hummelen, F. Wudl, A. J. Heeger, *Science* **1995**, *270*, 1789.
[2] J. J. M. Halls, C. A. Walsh, N. C. Greenham, E. A. Marseglia, R. H. Friend, S. C. Moratti, A. B. Holmes, *Nature* **1995**, *376*, 498.
[3] L. J. A. Koster, S. E. Shaheen, J. C. Hummelen, *Adv. Energy Mater.* **2012**, *2*, 1246.
[4] J. Guo, H. Ohkita, H. Benten, S. Ito, *J. Am. Chem. Soc.* **2010**, *132*, 6154.
[5] M. Lenes, L. J. A. Koster, V. D. Mihailetchi, P. W. M. Blom, *Appl. Phys. Lett.* **2006**, *88*, 243502.
[6] J.-W. van der Horst, P. A. Bobbert, P. H. L. de Jong, M. A. J. Michels, L. D. A. Siebbeles, J. M. Warman, G. H. Gelinck, G. Brocks, *Chem. Phys. Lett.* **2001**, *334*, 303.

[7] J. H. Choi, K.-I. Son, T. Kim, K. Kim, K. Ohkubo, S. Fukuzumi, *J. Mater. Chem.* **2010**, *20*, 475.
[8] D. Veldman, Ö. Ipek, S. C. J. Meskers, J. Sweelssen, M. M. Koetse, S. C. Veenstra, J. M. Kroon, S. S. van Bavel, J. Loos, R. a J. Janssen, *J. Am. Chem. Soc.* **2008**, *130*, 7721.
[9] M. a. Loi, S. Toffanin, M. Muccini, M. Forster, U. Scherf, M. Scharber, *Adv. Funct. Mater.* **2007**, *17*, 2111.
[10] B. Bernardo, D. Cheyns, B. Verreet, R. D. Schaller, B. P. Rand, N. C. Giebink, *Nat. Commun.* **2014**, *5*, 3245.
[11] A. Köhler, H. Bässler, *J. Mater. Chem.* **2011**, *21*, 4003.
[12] S. H. Park, A. Roy, S. Beaupré, S. Cho, N. Coates, J. S. Moon, D. Moses, M. Leclerc, K. Lee, A. J. Heeger, *Nat. Photonics* **2009**, *3*, 297.
[13] M. Breselge, I. Van Severen, L. Lutsen, P. Adriaensens, J. Manca, D. Vanderzande, T. Cleij, *Thin Solid Films* **2006**, *511*, 328.
[14] M. Lenes, F. B. Kooistra, J. C. Hummelen, I. Van Severen, L. Lutsen, D. Vanderzande, T. J. Cleij, P. W. M. Blom, *J. Appl. Phys.* **2008**, *104*, 114517.
[15] S. Y. Leblebici, T. L. Chen, P. Olalde-Velasco, W. Yang, B. Ma, *ACS Appl. Mater. Interfaces* **2013**, *5*, 10105.
[16] X. Liu, K. S. Jeong, B. P. Williams, K. Vakhshouri, C. Guo, K. Han, E. D. Gomez, Q. Wang, J. B. Asbury, *J. Phys. Chem. B* **2013**, *117*, 15866.
[17] R. J. Sengwa, *Polym. Int.* **1998**, *45*, 43.
[18] R. Sengwa, K. Kaur, R. Chaudhary, *Polym. Int.* **2000**, *49*, 599.
[19] M. F. Guest, I. J. Bush, H. J. J. van Dam, P. Sherwood, J. M. H. Thomas, J. H. van Lenthe, R. W. A. Havenith, J. Kendrick, *Mol. Phys.* **2005**, *103*, 719.
[20] F. Jensen, *Introduction to Computational Chemistry*, 2nd edition, John Wiley and Sons, Ltd, UK Chichester, **2007**, Ch. 13.
[21] D. F. Kronholm, J. C. Hummelen, A. B. Sieval, P. Van't Hof (Solenne BV), NL Patent 8435713 **2013.**
[22] F. Jahani, S. Torabi, R. C. Chiechi, L. J. A. Koster, J. C. Hummelen, *Chem. Commun.* **2014** ,*50* ,10645.
[23] a) C. Kanimozhi, N. Yaacobi-Gross, K. W. Chou, A. Amassian, T. D. Anthopoulos, S. Patil, *J. Am. Chem. Soc.* **2012**, *134*, 16532; b) C. Kanimozhi, N. Yaacobi-Gross,E. K. Burnett, A. L. Briseno, T. D. Anthopoulos, U. Salzner, S. Patil, *Phys. Chem. Chem. Phys.* **2014**, *16*, 17253.
[24] M. Pope, C. E. Swenberg, *Electronic Processes in Organic Crystals and Polymers*, Oxford University Press, NY USA, **1999**.
[25] E. Knapp, B. Ruhstaller, *J. Appl. Phys.* **2012**, *112*, 024519.
[26] J. Bisquert, G. Garcia-Belmonte, Á. Pitarch, H. J. Bolink, *Chem. Phys. Lett.* **2006**, *422*, 184.
[27] E. Ehrenfreund, C. Lungenschmied, G. Dennler, H. Neugebauer, N. S. Sariciftci, *Appl. Phys. Lett.* **2007**, *91*, 012112.
[28] V. Shrotriya, Y. Yang, *J. Appl. Phys.* **2005**, *97*, 054504.
[29] S. L. M. van Mensfoort, R. Coehoorn, *Phys. Rev. Lett.* **2008**, *100*, 086802.
[30] F. Liu, P. P. Ruden, I. H. Campbell, D. L. Smith, *Appl. Phys. Lett.* **2012**, *101*, 023501.
[31] P. N. Murgatroyd, *J Phys D: Appl Phys.* **1970**, *3*, 151.
[32] N. Craciun, J. Wildeman, P. Blom, *Phys. Rev. Lett.* **2008**, *100*, 056601.
[33] S. P. Senanayak, A. Z. Ashar, C. Kanimozhi, S. Patil, K. S. Narayan, unpublished.
[34] Y. Zhang, B. de Boer, P. W. M. Blom, *Phys. Rev. B* **2010**, *81*, 085201.